

Proton-detected ^{15}N - ^1H dipolar coupling/ ^1H chemical shift correlation experiment for the measurement of NH distances in biological solids under fast MAS solid-state NMR

Ekta Nehra^{1¶}, Neelam Sehrawat^{1¶}, Takeshi Kobayashi², Yusuke Nishiyama^{3,4*}, Manoj Kumar Pandey^{1*}

1 Indian Institute of Technology (IIT) Ropar, Rupnagar, Punjab, 140001, India

2 U.S. DOE, Ames Laboratory, Iowa State University, Ames, IA, 50011-3020, United States

3 RIKEN-JEOL Collaboration Center, RIKEN, Yokohama, Kanagawa, 230-0045, Japan

4 JEOL RESONANCE Inc., Musashino, Akishima, Tokyo, 196-8558, Japan

* Authors to whom correspondence should be addressed: mkpandey@iitrpr.ac.in, yunishiy@jeol.co.jp

¶ These authors contributed equally to this work

Abstract

Measurement of distances from dipolar couplings is essential for structural characterization, refinement and validation using the solid-state nuclear magnetic resonance (ssNMR) spectroscopy. Particularly, knowledge about NH dipolar interactions in biological solids is important for understanding the hydrogen (H)-bonding interactions, molecular geometry and spin dynamics. In this regard, we have proposed a proton-detected two-dimensional (2D) ^{15}N - ^1H dipolar coupling/ ^1H chemical shift correlation experiment using the C -symmetry based windowless recoupling of chemical shift anisotropy (ROCSA) in combination with the DIPSHIFT pulse-based method for the measurement of short NH distances in the isotopically labeled and naturally abundant biological solids at fast MAS rates (40-70 kHz). Our proposed method results in undistorted recoupled ^{15}N - ^1H dipolar coupling powder lineshapes that are free from the recoupled ^1H CSA contributions under the ^{15}N evolution, a feature that is essential for the measurement of NH distances with improved accuracy (± 500 Hz in terms of the NH dipolar couplings). The pulse sequence developed in the present study is also insensitive to the ^1H - ^1H homonuclear dipolar interactions, relaxation effects owing to its constant-time implementation, and t_1 -noise from the fluctuations in the magic angle spinning (MAS).

Introduction

Orientation dependent/anisotropic interactions like chemical shift anisotropy (CSA), dipolar and quadrupolar couplings in solid-state nuclear magnetic resonance (ssNMR) spectroscopy carry a variety of structural information at an atomic level. However, these interactions are partially or fully averaged out by magic angle spinning (MAS) used for a better site resolution and enhanced sensitivity of NMR spectra [1,2]. A careful manipulation of these interactions through the application of radio-frequency (rf) pulses in combination with MAS, commonly referred to as recoupling methods, holds the key for structural refinement and validation of chemical, materials and biological samples [3–11]. In such methods, the MAS averaged anisotropic interaction of choice is reintroduced by the application of rf pulses whose modulation frequency and/or field strengths are synchronized to MAS. In the recent past, methods to reintroduce the anisotropic interactions for structural constraints at fast MAS have gained considerable popularity in the magnetic resonance community thanks to improved sensitivity by the ^1H detection together with a minimal requirement of sample (~ 1 to 0.3 mg) [12–24].

While MAS rates > 40 kHz largely simplify problems related to the detection of protons, methods to measure the X- ^1H heteronuclear distances at such fast MAS rates are still emerging [25]. Previously, rotor-synchronized γ -encoded *R*-symmetry (RN_n^V) based 2D and 3D separated local field (SLF) and/or DIPSHIFT experiments were proposed to measure the $^{15}\text{N}/^{13}\text{C}$ - ^1H dipolar couplings in solid samples at variable MAS rates [26–35]. The conventional symmetry-based DIPSHIFT method was later modified by Hou et.al., and an elegant Phase-alternating *R*-Symmetry (PARS)-based method was proposed wherein phase-alternating *RN* blocks were applied on the ^1H channel along with an insertion of a π -pulse on the ^{15}N (^{13}C) channel at the end of every *RN* blocks for efficient suppression of ^1H CSAs under the X nuclei evolution [36,37]. The *R*-Symmetry-based Rotational Echo Double Resonance (S-REDOR) pulse sequence developed by Amoureux et.al., was used for ^{13}C - ^1H distance measurements in biological solids at 65 kHz MAS rate [38,39]. Nishiyama et.al. developed inversely detected Cross-Polarization with Variable Contact time (invCP-VC) method that was shown to provide accurate $^{13}\text{C}/^{15}\text{N}$ - ^1H short distances, and the method was used for the analysis of the dynamics in biological solids at fast MAS (≥ 60 kHz) [40,41]. For naturally abundant samples the phase-modulated symmetry-based rotational-echo

saturation-pulse double resonance (PM-S-RESPDOR) experiment was recently proposed for the measurement of ^{14}N - ^1H distances at fast MAS [42,43]. Nevertheless, several challenges as discussed below are associated with these experiments for the heteronuclear distance measurements at fast MAS.

Despite the robustness of the S-REDOR experiment at various experimental parameters, this method suffers from small fluctuations in the spinning frequency. As refocusing of the unwanted recoupled ^1H CSA is only completed at the end of the spin-echo duration, any fluctuations in the spinning frequency can lead to a loss in the S-REDOR signal efficiency. Subsequently, its implementation can be problematic at fast MAS wherein small fluctuations in the spinning frequency are generally unavoidable [44]. On the other hand, the unwanted recoupled ^1H CSA in the PARS approach is refocused during each cycle time of the symmetry element, therefore the method is essentially indifferent to the presence of ^1H CSA. Nevertheless, recoupled ^1H CSA in each sub-cycle can still contribute to the higher-order cross terms between the ^1H CSA and ^{15}N - ^1H dipolar-coupling operators. Moreover, the measurement of weaker X- ^1H dipolar couplings in the presence of a strong X- ^1H dipolar coupling using the PARS method is challenging due to the dipolar truncation. The CPVC method has also shown promising results for the accurate measurement of X- ^1H distances at fast MAS; however, its sensitivity towards the rf mismatch together with $T_{1\rho}$ decay can lead to a loss in the signal efficiency [45]. Furthermore, MAS rates > 60 kHz is mandatory as the extent of ^1H - ^1H decoupling is solely governed by the rate at which the sample spins. Also, this method assumes axially symmetric dipolar coupling tensor and therefore, can be challenging to study samples with intermediate correlation time and/or motionally averaged asymmetric tensors. The PM-S-RESPDOR method is advantageous owing to the high sensitivity resulting from the high natural abundance of ^{14}N . However, in the cases where multiple nitrogens appear in the vicinity of the target proton, the extraction of ^{14}N - ^1H distances becomes challenging in the presence of multiple ^{14}N - ^1H couplings, unlike in the ^{15}N -DIPSHIFT method. Although ^{14}N overtone REDOR alleviates this problem, well-separated overtone ^{14}N resonances are still essential in the experiment [46].

In this article, we propose a proton-detected 2D ^{15}N - ^1H dipolar coupling/ ^1H chemical shift (CS) correlation experiment using a C-symmetry-based windowless Recoupling of Chemical Shift Anisotropy (ROCSA) pulse sequence [47] in combination with the DIPSHIFT strategy that can potentially overcome most of the difficulties listed above.

We believe the proposed method can serve as an alternative to the existing methods used to measure short ^{15}N - ^1H distances at fast MAS. Previously, NH dipolar couplings have been utilized for relaxation-based dynamics studies using solution NMR and structural topology studies using static oriented bilayers [48,49]. Our focus in the present study is to measure short ^{15}N - ^1H distances in biological solids which can potentially be useful for probing the backbone and side-chain dynamics of peptides and proteins as well as to understand the H-bonding interactions responsible for protein folding and molecular recognition. Recently, the windowless ROCSA sequence was proposed by Kobayashi et.al., for the reintroduction of ^1H CSA at fast MAS [50]. This method allowed simultaneous recoupling of both the $|m| = 1$ and $|m| = 2$ spatial components of the ^1H CSA with complete suppression of the ^1H - ^1H homonuclear dipolar couplings thus facilitating the determination of both the sign and the magnitude of ^1H CSA. Since CSA and heteronuclear dipolar coupling have the same spatial and spin symmetries, both interactions are simultaneously reintroduced during the windowless ROCSA duration. This characteristic of the pulse sequence is exploited in the present study for the reintroduction of heteronuclear dipolar interactions. In the windowless ROCSA sequence, the ^1H CSA is reintroduced in the form of I_z operator, which commutes with the recoupled heteronuclear X- ^1H coupling operator ($I_z S_z$) and as the magnetization is brought onto the X-nuclei through the cross-polarization (CP) step, ^1H CSA does not interfere with the X- ^1H dipolar coupling under the X-nuclei evolution. Hence, the sequence is free from the ^1H CSA and can suppress the t_1 -noise caused by MAS fluctuations. Moreover, as the heteronuclear X- ^1H dipolar interactions between different spin pairs commute with each other, the ROCSA-based DIPSHIFT experiment can be designed and developed in the future to measure long-range correlations. The ROCSA-based DIPSHIFT method is also implemented in a constant-time manner to minimize any relaxation (T_2') effects or signal modulations due to the X spin CSA, X-X homonuclear dipolar and J couplings during the X- ^1H heteronuclear recoupling duration. With all the benefits of the ROCSA-based DIPSHIFT method listed above, we have demonstrated its applicability in the distance measurements in isotopically enriched and naturally abundant biological solids L-Histidine.HCl.H₂O (L-His.HCl.H₂O) and a tri-peptide, N-formyl-methionyl-leucyl-phenylalanine (MLF) at fast MAS rates (40-70 kHz).

Pulse Sequence

The proton-detected 2D ROCSA-based DIPSHIFT pulse sequence for the ^{15}N - ^1H dipolar coupling/ ^1H CS correlation experiment is shown in **Figure 1**. The initial 90° pulse on the ^1H channel creates the ^1H transverse magnetization which is then transferred to ^{15}N using a ramped amplitude-modulated cross-polarization (RAMP-CP) step. After the first CP step, the ^{15}N magnetization evolves for a constant echo duration T . A 180° pulse is inserted in the middle of the constant duration T to refocus ^{15}N isotropic chemical shifts. The ^{15}N - ^1H dipolar couplings are expressed during the incremental t_1 duration by an application of the rotor-synchronized C -symmetry based windowless ROCSA pulse sequence [$CN_n^\nu(90_0^\circ, 360_{180}^\circ, 540_0^\circ, 360_{180}^\circ, 90_0^\circ)$] with $N = 3$, $n = 3$ and $\nu = 1$] [50], henceforth referred to as the windowless $C3_3^1$ -ROCSA, followed by an application of a low power heteronuclear decoupling on the ^1H channel for the remaining echo duration $T-t_1$. Just after the constant duration T , the ^{15}N magnetization is stored along the z -direction by an application of a 90° pulse on the ^{15}N channel. The remnant transverse ^1H magnetization is removed by the application of the homonuclear rotary resonance (HORROR) sequence on the ^1H channel. The ^{15}N transverse magnetization is again created for the second CP transfer by an application of a 90° pulse on the ^{15}N channel and is transferred back to the protons during the RAMP-CP step for detection.

Experimental

All the NMR experiments on the labeled samples were carried out on a JEOL spectrometer (Model: JNM-ECZ600R, JEOL RESONANCE Inc., Japan) equipped with a 1.0 mm double-resonance (HX) fast MAS probe (JEOL RESONANCE Inc., Japan) and operating at the ^1H and ^{15}N Larmor frequencies of 599.672 and 60.764 MHz, respectively. For naturally abundant MLF, the 2D ^{15}N - ^1H dipolar coupling/ ^1H CS correlation experiment was performed on a JNM-ECZ900R spectrometer equipped with a 1.0 mm triple resonance probe (JEOL RESONANCE Inc. Japan) and operating at 899.4 MHz (^1H) and 91.1 MHz (^{15}N) Larmor frequencies. Approximately one mg powdered samples of $\text{U-}^{15}\text{N}$ L-His.HCl.H₂O, $\text{U-}^{15}\text{N}/^{13}\text{C}$ and naturally abundant MLF were separately packed into 1.0 mm zirconia rotors. A MAS rate (ν_r) of 69.832 kHz unless specified otherwise was used for all the NMR measurements conducted on the 600 MHz NMR spectrometer for the labeled samples at an ambient temperature. A MAS rate of 60.096 kHz was used for the NMR measurements on naturally abundant

MLF. Recycle delays of 7 s and 3 s were used for U-¹⁵N L-His.HCl.H₂O, and U-¹⁵N/¹³C and naturally abundant MLF, respectively. The 90° pulse lengths were optimized to 0.8 and 2.5 μs [600 MHz NMR spectrometer] and 1.03 and 2.42 μs [900 MHz NMR spectrometer] for ¹H and ¹⁵N, respectively. The double-quantum (DQ) Hartmann-Hahn CP matching condition [51] under MAS (¹H and ¹⁵N rf amplitudes of 19 kHz and 48 kHz [600 MHz NMR spectrometer], and 16 kHz and 46 kHz [900 MHz NMR spectrometer], respectively) was implemented in the RAMP-CP steps to avoid any sample heating due to the strong ¹H rf fields. While a longer contact time of 2 ms during the first CP step was used to maximize the magnetization transfer between ¹H and ¹⁵N, a shorter contact time of 0.4 ms was used in the second CP step to select directly bonded NH proton resonances. A ¹⁵N-¹H CW decoupling of the rf strengths ~9.1 kHz and 12 kHz was applied on the ¹H channel on 600 MHz and 900 MHz NMR spectrometers, respectively, during the duration $T-t_1$. The constant spin echo-time duration T in the experiment was set according to the relation [$T = 2\tau_r \times ((\text{maximum } t_1 \text{ increments} \times n) + 1)$; here, τ_r represents the rotor period]. A ¹⁵N-¹H WALTZ decoupling of the rf strengths ~8.6 kHz and 10 kHz was applied on the ¹⁵N channel on 600 and 900 MHz NMR spectrometers, respectively, during the ¹H acquisition period ($t_2 = 10.24$ ms). The phase-modulated (XYXY) HORROR sequence was applied for 200 ms with the ¹H rf field amplitude of 9.1 kHz and 7.3 kHz on 600 and 900 MHz NMR spectrometers, respectively. The windowless $C3_3^1$ -ROCSA pulse sequence for the recoupling of NH dipolar interactions was implemented with 32 t_1 time point increments for every 8, 32 and 4096 transients for U-¹⁵N L-His.HCl.H₂O, and U-¹⁵N/¹³C and naturally abundant MLF, respectively. Recoupled signals were obtained at every $6\tau_r$ unless specified otherwise with the rf field strengths 279.3 kHz and 240.4 kHz ($4\nu_r$) on 600 and 900 MHz NMR spectrometers, respectively. All the NMR data were processed using the Delta software (JEOL RESONANCE Inc.). The ¹⁵N-¹H dipolar coupling modulated time domain signal was processed using twelve times data zero filling followed by the real Fourier transform (FT). The recoupled experimental ¹⁵N-¹H dipolar coupling powder lineshapes were simulated with REPULSION678 (α, β) crystallite orientations and 60 γ -angles using the SIMPSON software [52–55]. A single exponential function with a line broadening of 150 Hz was applied before the FT of the dipolar modulated time domain data resulting from the simulations.

Results and Discussion

To highlight the role of unwanted ^1H CSA in the ^{15}N - ^1H distance measurements we carried out a systematic comparison of dipolar coupling powder lineshapes obtained from the existing γ -encoded R -symmetry-based DIPSHIFT methods with our proposed windowless $C3_3^1$ -ROCSA-based DIPSHIFT approach. In this regard, we performed two-spin (^1H and ^{15}N) numerical simulations using the SIMPSON software to generate the ^{15}N - ^1H coupling powder lineshapes from the γ -encoded R -symmetry-based $R16_3^2$ [32,56,57] and $R16_3^2$ -PARS with phase-alternating 180° pulses, and the windowless $C3_3^1$ -ROCSA based DIPSHIFT pulse sequences both in the presence and absence of a large ^1H CSA (-16.0 ppm), and a ^{15}N (S)- ^1H (I) dipolar coupling strength ($D_{IS} = b_{IS} / 2\pi = -\mu_0\gamma_I\gamma_S\hbar/8\pi^2 r_{IS}^3$) of 10 kHz. As shown in **Figure 2**, the reintroduced ^{15}N - ^1H dipolar coupling powder lineshapes from the γ -encoded $R16_3^2$ -based DIPSHIFT pulse sequence have a strong dependence on the ^1H CSA and the asymmetry parameter. The first-order average Hamiltonian [58–60] under the ^{15}N evolution in the case of γ -encoded symmetry-based sequences comprises of the ^1H CSA ($C_1I_+ + C_2I_-$; here C_1 and C_2 are ^1H CSA constants) and the ^{15}N - ^1H dipolar coupling ($C_3I_+S_z + C_4I_-S_z$; here C_3 and C_4 are ^{15}N - ^1H dipolar coupling constants) operators [61] which commute only if the γ -angles in their respective principal axes are considered to be the same. Generally, the ^1H CSA and ^{15}N - ^1H dipolar coupling operators in the first-order average Hamiltonian do not commute with each other and result in a huge distortion in the recoupled ^{15}N - ^1H dipolar coupling powder lineshape. Such a problem is alleviated by the implementation of PARS method that refocuses ^1H CSA every cycle time of the symmetry pulses and results in an undistorted recoupled ^{15}N - ^1H dipolar powder lineshape (**Figure 2**). Nevertheless, an appearance of the central peak at zero frequency due to the PARS method can contribute to a loss in recoupling efficiency/sensitivity and can interfere in the spectral analysis of smaller couplings. Moreover, the height of the central peak is pulse-sequence specific and can vary depending on the choice of the symmetry numbers. In contrast, the first-order average Hamiltonian for the windowless $C3_3^1$ -ROCSA-based DIPSHIFT method comprises of commuting longitudinal ^1H CSA (I_z) and the ^{15}N - ^1H dipolar coupling (I_zS_z) operators and therefore, the recoupled dipolar lineshapes should be unaffected from the ^1H CSA to the first-order. As shown in **Figure**

2 the windowless $C3_3^1$ -ROCSA-based DIPSHIFT method results in the ^{15}N - ^1H dipolar coupling powder lineshape which is largely unaffected by the presence of ^1H CSA under the ^{15}N evolution. Note that the recoupled dipolar coupling powder pattern is very similar to the static Pake doublet with two horns (internuclear dipolar coupling vector is perpendicular to the applied static magnetic field) together with foot signals (internuclear dipolar coupling vector is parallel to the applied static magnetic field). Minor deviation from the static Pake doublet can be attributed to the recoupling of dipolar Hamiltonian using the proposed pulse sequence in a slightly different form as compared to the static Hamiltonian. To further highlight the contributions from ^1H CSA and possible cross terms between the ^1H CSA and ^{15}N - ^1H dipolar couplings, we carried out numerical simulations using the windowless $C3_3^1$ -ROCSA-based DIPSHIFT pulse sequence with a variation of the ^{15}N - ^1H dipolar coupling strength from strong (10 kHz), medium (6 kHz) to weak (2 kHz) both in the presence and absence of a large ^1H CSA. As demonstrated in **Figure S1-a** of the supporting information, the ^{15}N - ^1H dipolar coupling powder lineshapes remain unaffected in the presence of ^1H CSA under the ^{15}N evolution highlighting their indifference to the ^1H CSA. Further we carried out a series of two-spin numerical simulations using the proposed pulse sequence and different magnitudes of the ^1H CSA (-20 ppm to 0 ppm) with an objective to understand the impact of changing magnitudes of ^1H CSA on the recoupled ^{15}N - ^1H dipolar coupling powder lineshapes under the ^{15}N evolution. Results emerging from the numerical simulations are shown in **Figure S1-b** of the supporting information. As evident the recoupled ^{15}N - ^1H dipolar coupling powder lineshapes remain invariant by the changing magnitudes of the ^1H CSA. The above observations emphasize the advantage of the windowless $C3_3^1$ -ROCSA-based DIPSHIFT experiment for the recoupling of heteronuclear dipolar couplings over the existing γ -encoded symmetry-based DIPSHIFT pulse methods including PARS.

To understand the multi-spin effects (^1H - ^1H homonuclear and long-range ^{15}N - ^1H heteronuclear dipolar interactions) of recoupling of one bond (short) ^{15}N - ^1H dipolar coupling using the windowless $C3_3^1$ -ROCSA-based DIPSHIFT pulse sequence, we carried out numerical simulations consisting of three (N-H2), four (N-H3) and five (N-H4) spins under the ^{15}N evolution at a fast MAS rate of 69.832 kHz. As depicted in **Figure S2** of the supporting information, the one bond ^{15}N - ^1H dipolar coupling powder

lineshapes remain invariant with the increase in the number of ^1H spins or the ^1H - ^1H homonuclear dipolar interactions in the absence of all the long-range NH dipolar couplings. In other words, the ^1H - ^1H homonuclear dipolar couplings contribute negligibly to the recoupled heteronuclear dipolar average Hamiltonian. To validate the role of long-range NH dipolar couplings in the estimation of one-bond (short) NH distances, we carried out numerical simulations with three (N-H2), four (N-H3) and five (N-H4) spins both in the presence and absence of all the long-range NH dipolar couplings under the ^{15}N evolution. The DIPSHIFT powder lineshape in principle should vary depending on the number and strengths of the long-range ^{15}N - ^1H dipolar couplings. Such effects can be seen in the multi-spin simulations (**Figure S3-a** of the supporting information) wherein contributions from the long-range NH dipolar interactions to the recoupled powder lineshapes are clearly visible especially at the foot of the powder pattern. As discussed above the recoupled dipolar coupling powder pattern exhibits pseudo-Pake doublet characteristic of a two-spin system, the presence of long-range interactions can only modify this powder pattern especially at the feet while retaining the separation between the two horns. Nevertheless, as the dipolar coupling singularities are retained, a two-spin model can in principle be used to extract the shortest ^{15}N - ^1H dipolar coupling. Theoretically, the DIPSHIFT spectra can be convoluted for the extraction of all the ^{15}N - ^1H dipolar couplings. Such an observation should lead to the design and development of windowless $C3_3^1$ -ROCSA-based DIPSHIFT experiments to measure long-range NH correlations relevant for structural studies [62]. We believe the time-domain data from the windowless $C3_3^1$ -ROCSA-based DIPSHIFT experiments can be utilized to separate the contributions from long-range and short-range dipolar couplings as demonstrated in the RESPDOR method [62]. This observation is in contrast to the PARS method wherein weak X- ^1H dipolar couplings cannot be measured in the presence of a strong X- ^1H dipolar coupling due to the dipolar truncation. Currently, we are in the process of exploring the possibility of measuring long-range NH dipolar couplings in our laboratory and results emerging from the study will be published elsewhere. Notably, all the multi-spin simulations depicted in **Figures S2 and S3-a** of the supporting information were carried out without the inclusion of ^1H CSAs i.e., a purely dipolar coupling Hamiltonian was considered. Though our proposed pulse sequence is shown to generate undistorted recoupled ^{15}N - ^1H dipolar coupling lineshapes in the presence of ^1H CSA from a two-spin model as

discussed above, it is important to check if the magnitude of the ^1H CSA or related higher-order cross-term contributions have any impact on the recoupled ^{15}N - ^1H dipolar coupling lineshapes when CSAs of protons are incorporated in the multi-spin simulations. In this regard, we carried out three, four and five spin simulations in the presence of ^1H CSAs and the results are plotted in **Figure S3-b** of the supporting information. As shown, the recoupled ^{15}N - ^1H dipolar coupling lineshapes remain unchanged in the presence of ^1H CSAs, which again confirms the fact that the proposed pulse sequence is tolerant to the presence of ^1H CSA. Any deviations in the ^{15}N - ^1H dipolar coupling lineshape from the two-spin model can be attributed to the long-range NH dipolar couplings as discussed above.

Figure 3 depicts the 2D ^{15}N - ^1H dipolar coupling/ ^1H CS correlation spectra of U- ^{15}N L-His.HCl.H₂O and U- $^{15}\text{N}/^{13}\text{C}$ MLF. The ^{15}N - ^1H dipolar coupling powder lineshapes for both the samples were extracted by taking slices parallel to the recoupled ^{15}N - ^1H dipolar dimension at the ^1H isotropic chemical shift values and are also shown in **Figure 3**. As demonstrated earlier through the numerical simulations, the experimental ^{15}N - ^1H dipolar coupling powder lineshapes extracted from the 2D ^{15}N - ^1H dipolar coupling/ ^1H CS correlation experiment are devoid of any central peak and therefore, simultaneous recoupling of the ^1H CSA has no effect on the recoupled dipolar coupling powder lineshapes under the ^{15}N evolution. The experimental ^{15}N - ^1H dipolar coupling powder lineshapes are fitted using the SIMPSON software to obtain the dipolar couplings. As shown in **Figure 3**, the experimental ^{15}N - ^1H dipolar coupling powder lineshapes match well with the numerical simulations. The dipolar coupling strengths obtained from the ^{15}N - ^1H dipolar coupling powder lineshape fittings are 9.67 kHz and 10.41 kHz for NH⁺ and NH groups in the imidazole ring of U- ^{15}N L-His.HCl.H₂O, respectively. The ^{15}N - ^1H dipolar couplings are converted to the NH distances as 1.079 Å and 1.054 Å for NH⁺ and NH groups, respectively, and are in close agreement with the results reported in the literature from the solid-state NMR studies [40,41]. The minor disagreement at the foot of the experimental and calculated patterns comes from the long-range ^{15}N - ^1H couplings. Estimated NH distances in the present study are slightly longer in comparison to the neutron diffraction study on L-His.HCl.H₂O wherein reported NH distances are 1.070 Å and 1.026 Å for NH⁺ and NH groups, respectively [63]. In general, NH distances measured from the solid-state NMR are shown to give longer distances [40,41] in comparison to neutron diffraction studies due to the impact of

liberation motion on dipolar couplings [49,64]. Similar to U-¹⁵N L-His.HCl.H₂O, the amide group ¹⁵N-¹H dipolar couplings were extracted for U-¹⁵N/¹³C MLF. The ¹⁵N-¹H dipolar coupling powder lineshape fittings resulted in 10.30 kHz, 10.30 kHz and 10.50 kHz, and the corresponding NH distances as 1.057 Å, 1.057 Å and 1.051 Å for the Leu-NH, Met-NH and Phe-NH groups, respectively. These values are in close agreement with those obtained with the invCPVC method (**Figure S4** of the supporting information) and reported earlier using the PARS method [36]. The NH distance associated with the NH₃⁺ group in U-¹⁵N L-His.HCl.H₂O could not be estimated due to poor sensitivity as the CP conditions were optimized for strongly dipolar coupled NH protons. This is attributed to the motionally averaged smaller NH dipolar couplings and contributions from the remote NH dipolar couplings to the powder lineshape. It is worthwhile mentioning that in the absence of sharply defined dipolar coupling singularities from the windowless C₃¹-ROCSA-based DIPSHIFT method, an error in the range of ± 500 Hz for the dipolar-coupling constant is inevitable. We have not used any software-based iterative lineshape-fitting tool and therefore, the error bar reported here is based on our judgment from the manual fitting. Deviations in the experimental and a model two-spin fitted dipolar coupling powder lineshapes from the numerical simulation can be mostly ascribed to the contributions from the remote ¹⁵N-¹H dipolar couplings as explained earlier. In addition, the CP transfer efficiencies may vary depending on the orientation of the NH bond with respect to the spinning axis that can also result in minor distortions in the experimental dipolar coupling powder lineshapes. For samples with overlapping ¹H resonances in the isotropic chemical shift dimension, a high-resolution ¹⁵N isotropic chemical shift (large chemical shift dispersion) dimension should be added to facilitate the extraction of ¹⁵N-¹H dipolar couplings through the ¹⁵N isotropic chemical shifts in addition to the ¹H shifts. In this regard, we designed the 3D ¹⁵N-¹H dipolar coupling/¹⁵N CS/¹H CS correlation pulse sequence with the windowless C₃¹-ROCSA-based DIPSHIFT unit for the reintroduction of ¹⁵N-¹H dipolar couplings (**Figure S5** of the supporting information). Notably, the ¹H resonances associated with the amide NH groups in U-¹⁵N/¹³C MLF are partially resolved and therefore, the 2D ¹⁵N-¹H dipolar /¹H CS correlation experiment may be sufficient to get information on the recoupled dipolar interactions. Nevertheless, we used U-¹⁵N/¹³C MLF for recording the 3D ¹⁵N-¹H dipolar/¹⁵N CS/¹H CS correlation experiment solely to test the working principles of the proposed pulse sequence. The

^{15}N - ^1H dipolar coupling powder lineshapes extracted from the 3D ^{15}N - ^1H dipolar coupling/ ^{15}N CS/ ^1H CS correlation data can be found in **Figure S5** of the supporting information. The ^{15}N - ^1H dipolar coupling powder lineshape fitting using SIMPSON resulted in 10.30 kHz, 10.00 kHz and 10.30 kHz, and the corresponding distances of 1.057 Å, 1.068 Å and 1.057 Å for the Leu-NH, Met-NH and Phe-NH groups, respectively. The estimated distances are comparable to those obtained from the 2D ^{15}N - ^1H dipolar coupling/ ^1H CS correlation experiment with the observed small differences well within the error limit.

To understand the role of rf mismatch on the sensitivity and dipolar splitting using the windowless $C3_3^1$ -ROCSA-based DIPSHIFT method, we collected a series of 2D ^{15}N - ^1H dipolar coupling/ ^1H CS correlation experiments with a variation of the rf amplitude of the windowless $C3_3^1$ -ROCSA pulses on $\text{U-}^{15}\text{N}$ L-His.HCl.H₂O sample. The rf amplitude of the windowless $C3_3^1$ -ROCSA pulses was varied from 80 % to 100 % of the maximum capability of the ^1H rf amplitude (302.4 kHz) in a step-size of 4 %. As depicted in **Figure 4**, the recoupled ^{15}N - ^1H dipolar coupling powder lineshapes for NH^+ and NH resonances of $\text{U-}^{15}\text{N}$ L-His.HCl.H₂O extracted from the 2D ^{15}N - ^1H dipolar coupling/ ^1H CS correlation experiments are sensitive to the rf mismatch. Both the intensity as well as the dipolar coupling splitting varies with the extent of rf mismatch. Therefore, it is important to calibrate the rf amplitude of the symmetry pulses before setting up the 2D ^{15}N - ^1H dipolar coupling/ ^1H CS correlation experiment. Nevertheless, the calibration of the rf amplitude for the symmetry pulses can simply be accomplished by running a set of nutation experiments with a variable ^1H 90° rf field strength using the ^1H - ^{15}N - ^1H double cross-polarization (DCP) pulse sequence [16] that forms the basic unit of the windowless $C3_3^1$ -ROCSA-based DIPSHIFT experiment. To achieve the actual B_1 field experienced by the sample, we collected nutation profiles with a variation of the initial ^1H 90° rf pulse amplitude (40 % to 100 % of the maximum rf capability in the step size of 10 %) in the DCP pulse sequence. The corresponding ^1H B_1 fields were calculated by taking an inverse of the difference of 3π and π pulse lengths or the 2π pulse length obtained from the nutation profiles. **Table-S1** in the supporting information has the information on the ^1H rf pulse parameters used for the calibration and calculation of the ^1H rf field (B_1). The calculated ^1H B_1 field strengths from the nutation profiles were plotted against the experimental ^1H 90° rf amplitudes and a linear

fit of the data points was obtained (**Figure S6** in the supporting information). From the linear fit equation ($y = mx + c$; where y-axis: observed B_1 field and x-axis: experimental ^1H rf amplitude supplied to the spectrometer) actual ^1H B_1 field can be calculated. For example, the ^1H B_1 field strength for the symmetry pulses in the windowless $C3_3^1$ -ROCSA-based DIPSHIFT is $4\nu_r$ (here ν_r is the MAS rate) = 279.3 kHz at a MAS rate of 69.832 kHz. Therefore, the corresponding rf amplitude from the calibration curve corresponds to 92% of the maximum capability of the ^1H rf amplitude.

To substantiate the role of MAS rate on the recoupled dipolar coupling powder lineshapes using the windowless $C3_3^1$ -ROCSA-based DIPSHIFT method, we carried out a series of the 2D ^{15}N - ^1H dipolar coupling/ ^1H CS correlation experiments at different MAS rates of 29.976, 40.064, 50.000 and 60.096 kHz and compared with the data recorded with a 69.832 kHz MAS rate. The main objective here was to explore the feasibility of the proposed method at MAS rates less than 65 kHz by observing the quality of the recoupled dipolar coupling powder pattern. The ^{15}N - ^1H dipolar coupling powder lineshapes extracted from the 2D ^{15}N - ^1H dipolar coupling/ ^1H CS correlation experiments on U- ^{15}N L-His.HCl.H₂O at different MAS rates are plotted in **Figure 5**. The ^{15}N - ^1H dipolar powder coupling lineshapes observed above 40 kHz are undistorted with well-defined singularities and are mostly free from the central peak, and match extremely well at all the MAS rates for both NH^+ and NH groups of the imidazole ring of U- ^{15}N L-His.HCl.H₂O. Such an observation highlights the robustness of the proposed method towards any higher-order contributions from the ^1H CSA and ^{15}N - ^1H dipolar coupling to the recoupled average Hamiltonian even at MAS rate ~ 40 kHz. However, the dipolar coupling powder lineshapes are slightly distorted and are also associated with a central peak in the case of the 2D ^{15}N - ^1H dipolar coupling/ ^1H CS correlation experiment at 29.976 kHz MAS rate. This spinning frequency may be considered as the lower limit for the implementation of the windowless $C3_3^1$ -ROCSA-based DIPSHIFT method for the ^{15}N - ^1H distance measurements.

Finally, we collected the 2D ^{15}N - ^1H dipolar coupling/ ^1H CS correlation experiment on a naturally abundant MLF using the windowless $C3_3^1$ -ROCSA-based DIPSHIFT method at fast MAS. Due to extremely low natural abundance (0.37%) and a small gyromagnetic ratio of the ^{15}N such an experimental analysis becomes challenging. Nevertheless, we can overcome such limitations through the proton detection method.

The 2D ^{15}N - ^1H dipolar coupling/ ^1H CS correlation spectrum of naturally abundant MLF is depicted in **Figure 6**. The experiment was recorded on a spectrometer operating at the ^1H Larmor frequency of 899.4 MHz under 60.096 kHz MAS rate with a large number of scans (4096) to achieve a good S/N ratio for the low naturally abundant ^{15}N . Spectral slices taken parallel to the ^{15}N - ^1H dipolar coupling dimension at the ^1H isotropic shifts of the Leu-NH, Met-NH and Phe-NH groups of MLF shows well separated dipolar singularities (**Figure 6**). The ^{15}N - ^1H dipolar powder coupling powder lineshape fitting from the SIMPSON software resulted in 10.3 and 10.0 Hz and 10.3 kHz, and the corresponding NH distances of 1.057 Å, 1.068 Å and 1.057 Å for the Leu-NH, Met-NH and Phe-NH groups, respectively. The ^{15}N - ^1H dipolar coupling constants for Leu-NH and Met-NH obtained for naturally abundant MLF agree well with the results from the U- $^{15}\text{N}/^{13}\text{C}$ MLF. The total experimental time (\sim 4.55 days) to record the 2D ^{15}N - ^1H dipolar/ ^1H CS correlation experiment is on a higher side and may act as a limitation of this approach for the naturally abundant samples. Nevertheless, a rapid repetition delay in biological solids may be achieved by a paramagnetic dopant [19].

Conclusion

To summarize we have proposed a proton-detected 2D ^{15}N - ^1H dipolar coupling/ ^1H CSA experiment recorded using a windowless $C3_3^1$ -ROCSA-based DIPSHIFT pulse sequence for the measurement of short ^{15}N - ^1H distances at fast MAS in a strongly coupled network of the proton spins. In the proposed method the ^{15}N - ^1H heteronuclear dipolar couplings are reintroduced without distortion and the dipolar coupling powder lineshapes are devoid of contributions from the ^1H CSA, the ^1H - ^1H homonuclear dipolar interactions, t_1 noise, relaxation, multi-spin (in the absence of long-range NH couplings) and higher-order effects. The ^{15}N - ^1H distances extracted using the proposed method are in good agreement with the values reported in earlier literature. We believe the proposed method has every potential to become a method of choice to accurately measure ^{15}N - ^1H distances and to probe local molecular dynamics in more complex biological systems at fast MAS.

Declaration of competing interest

The authors declare that they have no known competing financial interests or personal relationships that could have appeared to influence the work reported in this paper.

Acknowledgments

M.K.P. would like to acknowledge the Science and Engineering Research Board (SERB)-Department of Science and Technology (DST), Government of India (SERB-DST Grant ECR/2017/000713) and IIT Ropar for the financial support. E.N. and N.S. would like to acknowledge IIT Ropar for the graduate assistantship. This work was supported by JSPS KAKENHI Grant Number 20K05483 and in part by the JST-Mirai Program (Grant No. JPMJMI17A2, Japan) to Y. N. This work was partly supported by the U.S. Department of Energy (DOE), Office of Science, Basic Energy Sciences, Materials Science and Engineering Division to T.K. The Ames Laboratory is operated for the DOE by Iowa State University under contract No. DE-AC02-07CH11358 (TK).

References:

- [1] I.J. Lowe, Free induction decays of rotating solids., *Physical Review Letters*. 2 (1959) 285–287. <https://doi.org/10.1103/PhysRevLett.2.285>.
- [2] E.R. Andrew, A. Bradbury, R.G. Eades, Removal of Dipolar Broadening of Nuclear Magnetic Resonance Spectra of Solids by Specimen Rotation, *Nature*. 183 (1959) 1802–1803. <https://doi.org/10.1038/1831802a0>.
- [3] A.E. Bennett, C.M. Rienstra, J.M. Griffiths, W. Zhen, P.T. Lansbury, R.G. Griffin, Homonuclear radio frequency-driven recoupling in rotating solids, *Journal of Chemical Physics*. 108 (1998) 9463–9479. <https://doi.org/10.1063/1.476420>.
- [4] M. Baldus, D.G. Geurts, B.H. Meier, Broadband dipolar recoupling in rotating solids: A numerical comparison of some pulse schemes, *Solid State Nuclear Magnetic Resonance*. 11 (1998) 157–168. [https://doi.org/10.1016/S0926-2040\(98\)00036-8](https://doi.org/10.1016/S0926-2040(98)00036-8).
- [5] J.D. Gross, D.E. Warschawski, R.G. Griffin, Dipolar recoupling in MAS NMR: A probe for segmental order in lipid bilayers, *Journal of the American Chemical Society*. 119 (1997) 796–802. <https://doi.org/10.1021/ja962951b>.
- [6] S. Dusold, A. Sebald, Dipolar recoupling under magic-angle spinning conditions, *Annual Reports on NMR Spectroscopy*. 41 (2000) 185–264. [https://doi.org/10.1016/s0066-4103\(00\)41010-0](https://doi.org/10.1016/s0066-4103(00)41010-0).
- [7] R.G. Griffin, Dipolar recoupling in MAS spectra of biological solids, *Nature Structural Biology*. 5 (1998) 508–512. <https://doi.org/10.1038/749>.
- [8] M.H. Levitt, T.G. Oas, R.G. Griffin, Rotary Resonance Recoupling in Heteronuclear Spin Pair Systems, *Israel Journal of Chemistry*. 28 (1988) 271–282. <https://doi.org/10.1002/ijch.198800039>.
- [9] G. De Paepe, Dipolar Recoupling in Magic Angle Spinning Solid-State Nuclear Magnetic Resonance, *Annual Review of Physical Chemistry*. 63 (2012) 661–684. <https://doi.org/10.1146/annurev-physchem-032511-143726>.
- [10] S.O. Smith, Magic angle spinning NMR methods for internuclear distance measurements, *Current Opinion in Structural Biology*. 3 (1993) 755–759. [https://doi.org/10.1016/0959-440X\(93\)90060-X](https://doi.org/10.1016/0959-440X(93)90060-X).
- [11] U. Sivarajan, R. Ramachandran, Unraveling multi-spin effects in rotational resonance nuclear magnetic resonance using effective reduced density matrix theory, *Journal of Chemical Physics*. 140 (2014) 054101.

<https://doi.org/10.1063/1.4863212>.

- [12] H.R.W. Dannatt, G.F. Taylor, K. Varga, V.A. Higman, M.P. Pfeil, L. Asilmovska, P.J. Judge, A. Watts, ^{13}C - and ^1H -detection under fast MAS for the study of poorly available proteins: Application to sub-milligram quantities of a seven trans-membrane protein, *Journal of Biomolecular NMR*. 62 (2015) 17–23. <https://doi.org/10.1007/s10858-015-9911-1>.
- [13] M.K. Pandey, J.T. Damron, A. Ramamoorthy, Y. Nishiyama, Proton-detected 3D ^1H anisotropic/ ^{14}N / ^1H isotropic chemical shifts correlation NMR under fast magic angle spinning on solid samples without isotopic enrichment, *Solid State Nuclear Magnetic Resonance*. 97 (2019) 40–45. <https://doi.org/10.1016/j.ssnmr.2018.12.002>.
- [14] N.T. Duong, S. Raran-Kurussi, Y. Nishiyama, V. Agarwal, Quantitative ^1H - ^1H Distances in Protonated Solids by Frequency-Selective Recoupling at Fast Magic Angle Spinning NMR, *Journal of Physical Chemistry Letters*. 9 (2018) 5948–5954. <https://doi.org/10.1021/acs.jpcclett.8b02189>.
- [15] Y. Ji, L. Liang, X. Bao, G. Hou, Recent progress in dipolar recoupling techniques under fast MAS in solid-state NMR spectroscopy, *Solid State Nuclear Magnetic Resonance*. 112 (2021) 101711. <https://doi.org/10.1016/j.ssnmr.2020.101711>.
- [16] Y. Nishiyama, Fast magic-angle sample spinning solid-state NMR at 60–100 kHz for natural abundance samples, *Solid State Nuclear Magnetic Resonance*. 78 (2016) 24–36. <https://doi.org/10.1016/j.ssnmr.2016.06.002>.
- [17] Y. Ishii, A. Wickramasinghe, I. Matsuda, Y. Endo, Y. Ishii, Y. Nishiyama, T. Nemoto, T. Kamihara, Progress in proton-detected solid-state NMR (SSNMR): Super-fast 2D SSNMR collection for nano-mole-scale proteins, *Journal of Magnetic Resonance*. 286 (2018) 99–109. <https://doi.org/10.1016/j.jmr.2017.11.011>.
- [18] S. Asami, B. Reif, Proton-detected solid-state NMR spectroscopy at aliphatic sites: Application to crystalline systems, *Accounts of Chemical Research*. 46 (2013) 2089–2097. <https://doi.org/10.1021/ar400063y>.
- [19] S. Parthasarathy, Y. Nishiyama, Y. Ishii, Sensitivity and Resolution Enhanced Solid-State NMR for Paramagnetic Systems and Biomolecules under Very Fast Magic Angle Spinning., *Accounts of Chemical Research*. 46 (2013) 2127–2135. <https://doi.org/10.1021/ar4000482>.

- [20] D.H. Zhou, G. Shah, M. Cormos, C. Mullen, D. Sandoz, C.M. Rienstra, Proton-Detected Solid-State NMR Spectroscopy of Fully Protonated Proteins at 40 kHz Magic-Angle Spinning, *Journal of the American Chemical Society*. 129 (2007) 11791–11801. <https://doi.org/10.1021/ja073462m>.
- [21] G. Kervern, G. Pintacuda, Y. Zhang, E. Oldfield, C. Roukoss, E. Kuntz, E. Herdtweck, J.M. Basset, S. Cadars, A. Lesage, C. Copéret, L. Emsley, Solid-state NMR of a paramagnetic DIAD-Fe(II) catalyst: Sensitivity, resolution enhancement, and structure-based assignments, *Journal of the American Chemical Society*. 128 (2006) 13545–13552. <https://doi.org/10.1021/ja063510n>.
- [22] V. Agarwal, S. Penzel, K. Szekely, R. Cadalbert, E. Testori, A. Oss, J. Past, A. Samoson, M. Ernst, A. Böckmann, B.H. Meier, De Novo 3D Structure Determination from Sub-milligram Protein Samples by Solid-State 100kHz MAS NMR Spectroscopy, *Angewandte Chemie - International Edition*. 53 (2014) 12253–12256. <https://doi.org/10.1002/anie.201405730>.
- [23] D. Cala-De Paepe, J. Stanek, K. Jaudzems, K. Tars, L.B. Andreas, G. Pintacuda, Is protein deuteration beneficial for proton detected solid-state NMR at and above 100 kHz magic-angle spinning?, *Solid State Nuclear Magnetic Resonance*. 87 (2017) 126–136. <https://doi.org/10.1016/j.ssnmr.2017.07.004>.
- [24] M. Schledorn, A.A. Malär, A. Torosyan, S. Penzel, D. Klose, A. Oss, M.-L. Org, S. Wang, L. Lecoq, R. Cadalbert, A. Samoson, A. Böckmann, B.H. Meier, Protein NMR Spectroscopy at 150 kHz Magic-Angle Spinning Continues To Improve Resolution and Mass Sensitivity., *Chembiochem*. 21 (2020) 2540–2548. <https://doi.org/10.1002/cbic.202000341>.
- [25] L. Liang, Y. Ji, Z. Zhao, C.M. Quinn, X. Han, X. Bao, T. Polenova, G. Hou, Accurate heteronuclear distance measurements at all magic-angle spinning frequencies in solid-state NMR spectroscopy, *Chemical Science*. 12 (2021) 11554–11564. <https://doi.org/10.1039/d1sc03194e>.
- [26] S. V. Dvinskikh, H. Zimmermann, A. Maliniak, D. Sandström, Measurements of motionally averaged heteronuclear dipolar couplings in MAS NMR using R-type recoupling, *Journal of Magnetic Resonance*. 168 (2004) 194–201. <https://doi.org/10.1016/j.jmr.2004.03.001>.
- [27] S. V. Dvinskikh, Z. Luz, H. Zimmermann, A. Maliniak, D. Sandström, Molecular characterization of hexaoctyloxy-rufigallol in the solid and columnar

- phases: A local field NMR study, *Journal of Physical Chemistry B*. 107 (2003) 1969–1976. <https://doi.org/10.1021/jp0274381>.
- [28] R.K. Hester, J.L. Ackerman, B.L. Neff, J.S. Waugh, Separated Local Field Spectra in NMR: Determination of Structure of Solids, *Physical Review Letters*. 36 (1976) 1081–1083. <https://doi.org/10.1103/PhysRevLett.36.1081>.
- [29] M.E. Stoll, A.J. Vega, R.W. Vaughan, Heteronuclear dipolar modulated chemical shift spectra for geometrical information in polycrystalline solids, *The Journal of Chemical Physics*. 65 (1976) 4093–4098. <https://doi.org/10.1063/1.432863>.
- [30] G. Hou, S. Paramasivam, S. Yan, T. Polenova, A.J. Vega, Multidimensional magic angle spinning NMR spectroscopy for site-resolved measurement of proton chemical shift anisotropy in biological solids, *Journal of the American Chemical Society*. 135 (2013) 1358–1368. <https://doi.org/10.1021/ja3084972>.
- [31] M.H. Levitt, Symmetry-Based Pulse Sequences in Magic-Angle Spinning Solid-State NMR, in: *ChemInform*, 2003: pp. 165–196. <https://doi.org/10.1002/chin.200338276>.
- [32] G. Hou, I.J.L. Byeon, J. Ahn, A.M. Gronenborn, T. Polenova, ^1H - $^{13}\text{C}/^1\text{H}$ - ^{15}N heteronuclear dipolar recoupling by R-symmetry sequences under fast magic angle spinning for dynamics analysis of biological and organic solids, *Journal of the American Chemical Society*. 133 (2011) 18646–18655. <https://doi.org/10.1021/ja203771a>.
- [33] M.G. Munowitz, R.G. Griffin, Two-dimensional nuclear magnetic resonance in rotating solids: Time reversal effects in chemical shift-dipolar spectra, *The Journal of Chemical Physics*. 78 (1982) 613–617. <https://doi.org/10.1063/1.444816>.
- [34] M.G. Munowitz, R.G. Griffin, G. Bodenhausen, T.H. Huang, Two-Dimensional Rotational Spin-Echo Nuclear Magnetic Resonance in Solids: Correlation of Chemical Shift and Dipolar Interactions, *Journal of the American Chemical Society*. 103 (1981) 2529–2533. <https://doi.org/10.1021/ja00400a007>.
- [35] E.R. DeAzevedo, K. Saalwachter, O. Pascui, A.A. De Souza, T.J. Bonagamba, D. Reichert, Intermediate motions as studied by solid-state separated local field NMR experiments, *Journal of Chemical Physics*. 128 (2008) 104505. <https://doi.org/10.1063/1.2831798>.

- [36] G. Hou, X. Lu, A.J. Vega, T. Polenova, Accurate measurement of heteronuclear dipolar couplings by phase-alternating R-symmetry (PARS) sequences in magic angle spinning NMR spectroscopy, *Journal of Chemical Physics*. 141 (2014) 104202. <https://doi.org/10.1063/1.4894226>.
- [37] X. Lu, H. Zhang, M. Lu, A.J. Vega, G. Hou, T. Polenova, Improving dipolar recoupling for site-specific structural and dynamics studies in biosolids NMR: Windowed RN-symmetry sequences, *Physical Chemistry Chemical Physics*. 18 (2016) 4035–4044. <https://doi.org/10.1039/c5cp07818k>.
- [38] L. Chen, Q. Wang, B. Hu, O. Lafon, J. Trébosc, F. Deng, J.P. Amoureux, Measurement of hetero-nuclear distances using a symmetry-based pulse sequence in solid-state NMR, *Physical Chemistry Chemical Physics*. 12 (2010) 9395–9405. <https://doi.org/10.1039/b926546e>.
- [39] Q. Wang, X. Lu, O. Lafon, J. Trébosc, F. Deng, B. Hu, Q. Chen, J.P. Amoureux, Measurement of ^{13}C - ^1H dipolar couplings in solids by using ultra-fast magic-angle spinning NMR spectroscopy with symmetry-based sequences, *Physical Chemistry Chemical Physics*. 13 (2011) 5967–5973. <https://doi.org/10.1039/c0cp01907k>.
- [40] Y. Nishiyama, M. Malon, M.J. Potrzebowski, P. Paluch, J.P. Amoureux, Accurate NMR determination of C-H or N-H distances for unlabeled molecules, *Solid State Nuclear Magnetic Resonance*. 73 (2016) 15–21. <https://doi.org/10.1016/j.ssnmr.2015.06.005>.
- [41] P. Paluch, T. Pawlak, J.P. Amoureux, M.J. Potrzebowski, Simple and accurate determination of X-H distances under ultra-fast MAS NMR, *Journal of Magnetic Resonance*. 233 (2013) 56–63. <https://doi.org/10.1016/j.jmr.2013.05.005>.
- [42] S.A. Southern, D.L. Bryce, “Recent advances in nmr crystallography and polymorphism,” *Annual Reports on NMR Spectroscopy*. 102 (2021) 1–62. <https://doi.org/10.1016/bs.arnmr.2020.10.001>.
- [43] N.T. Duong, F. Rossi, M. Makrinich, A. Goldbourt, M.R. Chierotti, R. Gobetto, Y. Nishiyama, Accurate ^1H - ^{14}N distance measurements by phase-modulated RESPDOR at ultra-fast MAS, *Journal of Magnetic Resonance*. 308 (2019) 106559. <https://doi.org/10.1016/j.jmr.2019.07.046>.
- [44] X. Lu, O. Lafon, J. Trébosc, J.P. Amoureux, Detailed analysis of the S-RESPDOR solid-state NMR method for inter-nuclear distance measurement

- between spin-1/2 and quadrupolar nuclei, *Journal of Magnetic Resonance*. 215 (2011) 34–49. <https://doi.org/10.1016/j.jmr.2011.12.009>.
- [45] P. Paluch, J. Trébosc, Y. Nishiyama, M.J. Potrzebowski, M. Malon, J.P. Amoureux, Theoretical study of CP-VC: A simple, robust and accurate MAS NMR method for analysis of dipolar C-H interactions under rotation speeds faster than ca. 60 kHz, *Journal of Magnetic Resonance*. 252 (2015) 67–77. <https://doi.org/10.1016/j.jmr.2015.01.002>.
- [46] N.T. Duong, Z. Gan, Y. Nishiyama, Selective ^1H - ^{14}N Distance Measurements by ^{14}N Overtone Solid-State NMR Spectroscopy at Fast MAS, *Frontiers in Molecular Biosciences*. 8 (2021) 1–13. <https://doi.org/10.3389/fmolb.2021.645347>.
- [47] J.C.C. Chan, R. Tycko, Recoupling of chemical shift anisotropies in solid-state NMR under high-speed magic-angle spinning and in uniformly ^{13}C -labeled systems, *Journal of Chemical Physics*. 118 (2003) 8378–8389. <https://doi.org/10.1063/1.1565109>.
- [48] S.J. Opella, F.M. Marassi, Applications of NMR to membrane proteins, *Archives of Biochemistry and Biophysics*. 628 (2017) 92–101. <https://doi.org/10.1016/j.abb.2017.05.011>.
- [49] A. Ramamoorthy, C.H. Wu, S.J. Opella, Magnitudes and orientations of the principal elements of the ^1H chemical shift, ^1H - ^{15}N dipolar coupling, and ^{15}N chemical shift interaction tensors in $^{15}\text{N}_{\epsilon 1}$ -tryptophan and $^{15}\text{N}_{\pi}$ -histidine side chains determined by Three-Dimensional Solid-State NMR Spectroscopy of Polycrystalline Samples, *Journal of the American Chemical Society*. 119 (1997) 10479–10486. <https://doi.org/10.1021/ja9632670>.
- [50] T. Kobayashi, F.A. Perras, Y. Nishiyama, Determination of the chemical shift tensor anisotropy and asymmetry of strongly dipolar coupled protons under fast MAS, *Solid State Nuclear Magnetic Resonance*. 114 (2021) 101743. <https://doi.org/10.1016/j.ssnmr.2021.101743>.
- [51] B.H. Meier, Cross polarization under fast magic angle spinning: thermodynamical considerations, *Chemical Physics Letters*. 188 (1992) 201–207. [https://doi.org/10.1016/0009-2614\(92\)90009-C](https://doi.org/10.1016/0009-2614(92)90009-C).
- [52] M. Bak, N.C. Nielsen, Repulsion, A Novel Approach to Efficient Powder Averaging in Solid-State NMR, *Journal of Magnetic Resonance*. 125 (1997) 132–139. <https://doi.org/10.1006/jmre.1996.1087>.

- [53] M. Bak, J.T. Rasmussen, N.C. Nielsen, SIMPSON: A general simulation program for solid-state NMR spectroscopy, *Journal of Magnetic Resonance*. 147 (2000) 296–330. <https://doi.org/10.1006/jmre.2000.2179>.
- [54] Z. Tošner, R. Andersen, B. Stevansson, M. Edén, N.C. Nielsen, T. Vosegaard, Computer-intensive simulation of solid-state NMR experiments using SIMPSON, *Journal of Magnetic Resonance*. 246 (2014) 79–93. <https://doi.org/10.1016/j.jmr.2014.07.002>.
- [55] D.W. Juhl, Z. Tošner, T. Vosegaard, Versatile NMR simulations using SIMPSON, *Annual Reports on NMR Spectroscopy*. 100 (2020) 1–59. <https://doi.org/10.1016/bs.arnmr.2019.12.001>.
- [56] M.K. Pandey, M. Malon, A. Ramamoorthy, Y. Nishiyama, Composite-180° pulse-based symmetry sequences to recouple proton chemical shift anisotropy tensors under ultrafast MAS solid-state NMR spectroscopy, *Journal of Magnetic Resonance*. 250 (2015) 45–54. <https://doi.org/10.1016/j.jmr.2014.11.002>.
- [57] H.K. Miah, D.A. Bennett, D. Iuga, J.J. Titman, Measuring proton shift tensors with ultrafast MAS NMR, *Journal of Magnetic Resonance*. 235 (2013) 1–5. <https://doi.org/10.1016/j.jmr.2013.07.005>.
- [58] U. Haeberlen, J.S. Waugh, Coherent Averaging Effects in Magnetic Resonance., *Physical Review*. 175 (1968) 453–467. <https://doi.org/10.1103/PhysRev.175.453>.
- [59] M.M. Maricq, J.S. Waugh, NMR in rotating solids, *The Journal of Chemical Physics*. 70 (1979) 3300–3316. <https://doi.org/10.1063/1.437915>.
- [60] A. Brinkmann, Introduction to average Hamiltonian theory. I. Basics, Concepts in *Magnetic Resonance Part A*. 45 (2016) 1–19. <https://doi.org/10.1002/cmr.a.21414>.
- [61] X. Zhao, M. Edén, M.H. Levitt, Recoupling of heteronuclear dipolar interactions in solid-state NMR using symmetry-based pulse sequences, *Chemical Physics Letters*. 342 (2001) 353–361. [https://doi.org/10.1016/S0009-2614\(01\)00593-0](https://doi.org/10.1016/S0009-2614(01)00593-0).
- [62] N.T. Duong, Y. Aoyama, K. Kawamoto, T. Yamazaki, Y. Nishiyama, Structure Solution of Nano-Crystalline Small Molecules Using MicroED and Solid-State NMR Dipolar-Based Experiments., *Molecules*. 26 (2021) 4652. <https://doi.org/10.3390/molecules26154652>.

- [63] H. Fuess, D. Hohlwein, S.A. Mason, Neutron Diffraction Study of L-Histidine Hydrochloride Monohydrate, *Acta Crystallographica Section B*. B33 (1977) 654–659. <https://doi.org/https://doi.org/10.1107/S0567740877004415>.
- [64] Y. Ishii, T. Terao, S. Hayashi, Theory and simulation of vibrational effects on structural measurements by solid-state nuclear magnetic resonance, *Journal of Chemical Physics*. 107 (1997) 2760–2774. <https://doi.org/10.1063/1.474633>.

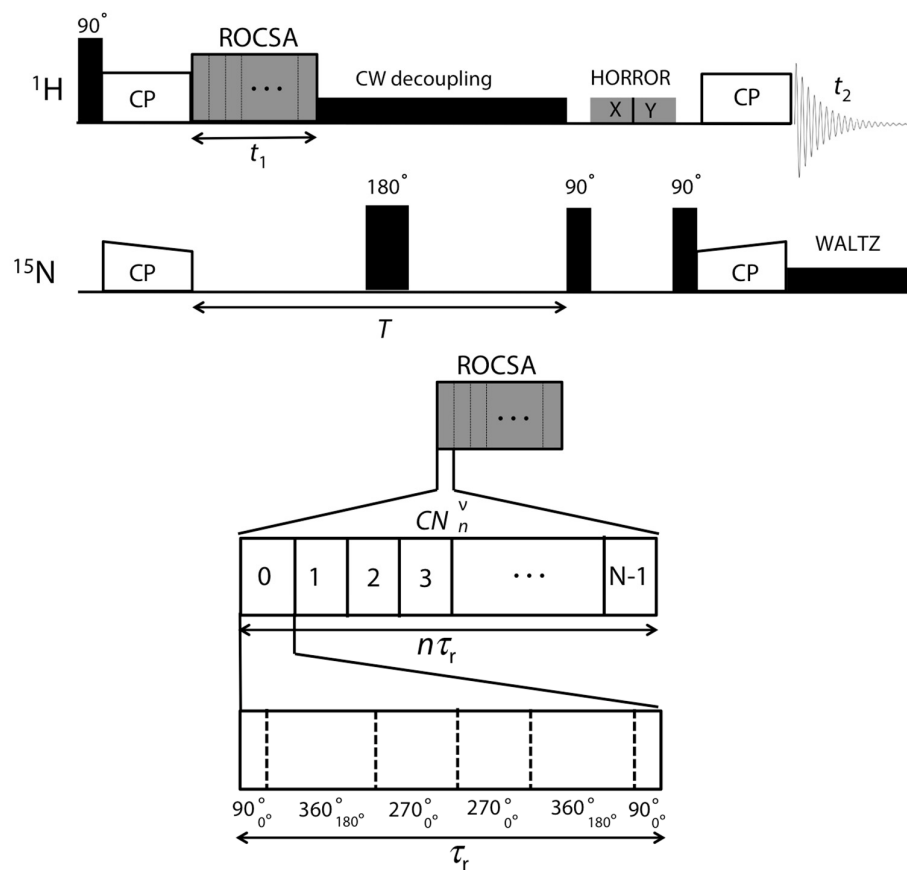


Figure 1: Proton-detected 2D windowless ROCSA-based DIPSHIFT pulse sequence for the measurement of NH dipolar couplings/distances through ^{15}N - ^1H dipolar coupling/ ^1H CS correlations.

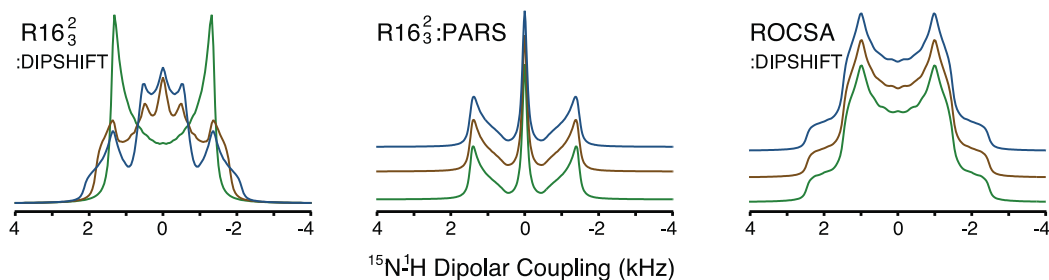


Figure 2: Two-spin (^1H and ^{15}N) SIMPSON simulations using the γ -encoded R -symmetry-based $R16_3^2$ and $R16_3^2$ -PARS with phase alternating 180° pulses, and the proposed windowless $C3_3^1$ -ROCSA-based DIPSHIFT pulse sequences to depict the role of unwanted ^1H CSA in the recoupled heteronuclear dipolar interactions under the ^{15}N evolution. The simulations were carried out without (green) and with ^1H CSA = -16.0 ppm and $\eta = 0.0$ (brown) and $\eta = 1.0$ (blue) under the MAS rate of 69.832 kHz at the ^1H Larmor frequency of 600 MHz. In all the simulations I (^1H)- S (^{15}N)-dipolar coupling strength ($D_{IS} = b_{IS} / 2\pi = -\mu_0\gamma_I\gamma_S\hbar/8\pi^2 r_{IS}^3$) was 10 kHz, and the ^{15}N - ^1H dipolar and the ^1H CSA principal axis system (PAS) angles were $(0, \beta_{\text{dip}}=30^\circ, 0)$ and $(0, 0, 0)$, respectively.

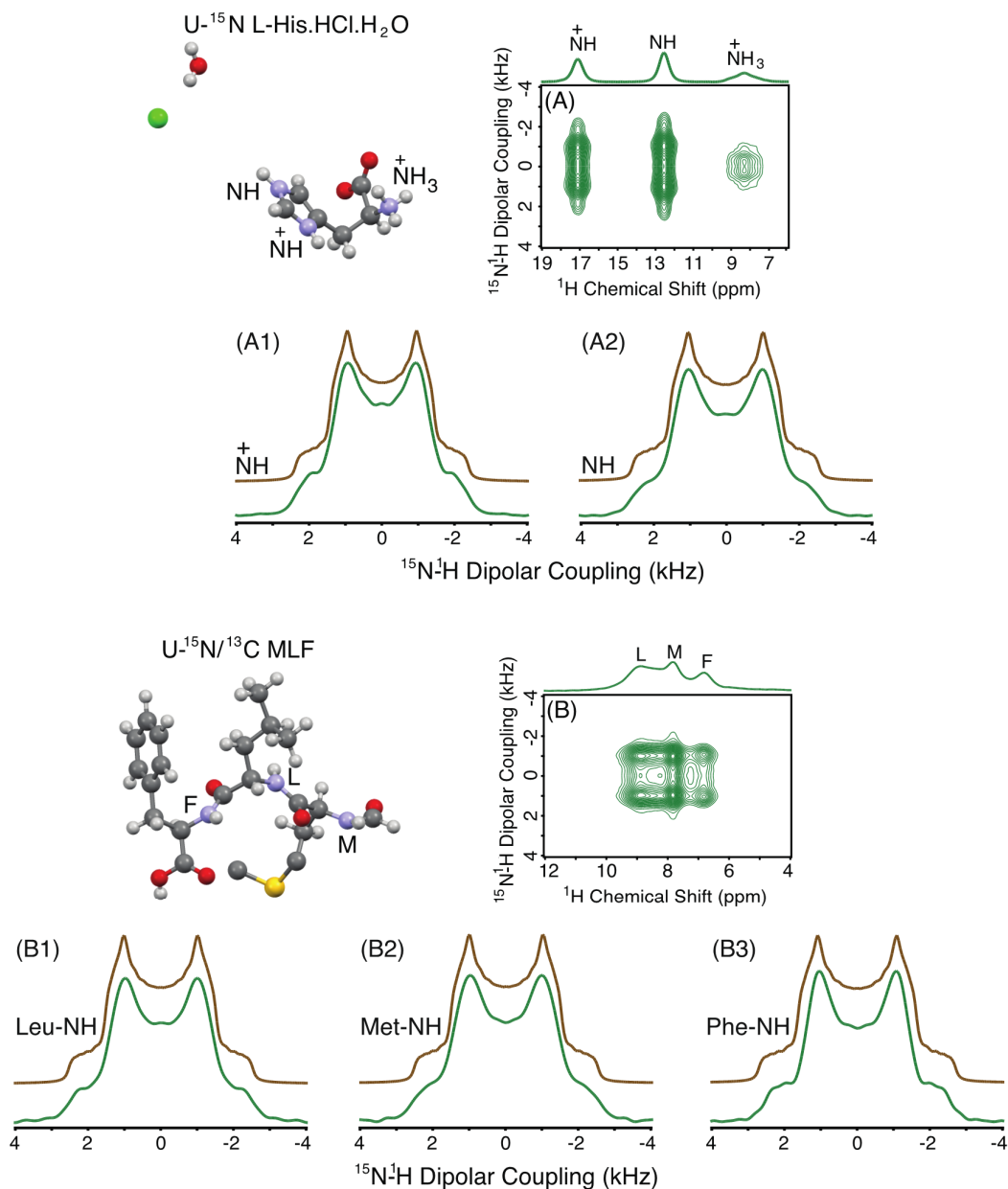


Figure 3: Chemical structures and 2D ^{15}N - ^1H dipolar coupling/ ^1H CS correlation spectra of U- ^{15}N L-His.HCl.H $_2\text{O}$ (A) and U- $^{15}\text{N}/^{13}\text{C}$ MLF (B) recorded by implementing the windowless $C3_3^1$ -ROCSA-based DIPSHIFT pulse sequence at the ^1H Larmor frequency of 600 MHz under 69.832 kHz MAS rate. One-dimensional (1D) projections of the dipolar/CS correlation spectra are shown onto their respective ^1H chemical shift axes. Below the 2D ^{15}N - ^1H dipolar coupling/ ^1H CS spectra shown are the experimental (green) ^{15}N - ^1H dipolar powder lineshapes extracted from the 2D dipolar coupling/CS correlation spectra of U- ^{15}N L-His.HCl.H $_2\text{O}$ [NH $_3^+$ (A1), NH (A2)]

and U- $^{15}\text{N}/^{13}\text{C}$ MLF [Leu-NH (B1), Met-NH (B2), Phe-NH (B3)]. The ^{15}N - ^1H dipolar coupling powder lineshapes were extracted by taking spectral slices parallel to the NH dipolar-recoupling dimension of the 2D ^{15}N - ^1H dipolar coupling/ ^1H CS correlation spectra at respective ^1H isotropic chemical shifts. Best-fitted simulated ^{15}N - ^1H dipolar coupling powder lineshapes using a two-spin (^1H - ^{15}N) model from the SIMPSON software are shown in brown.

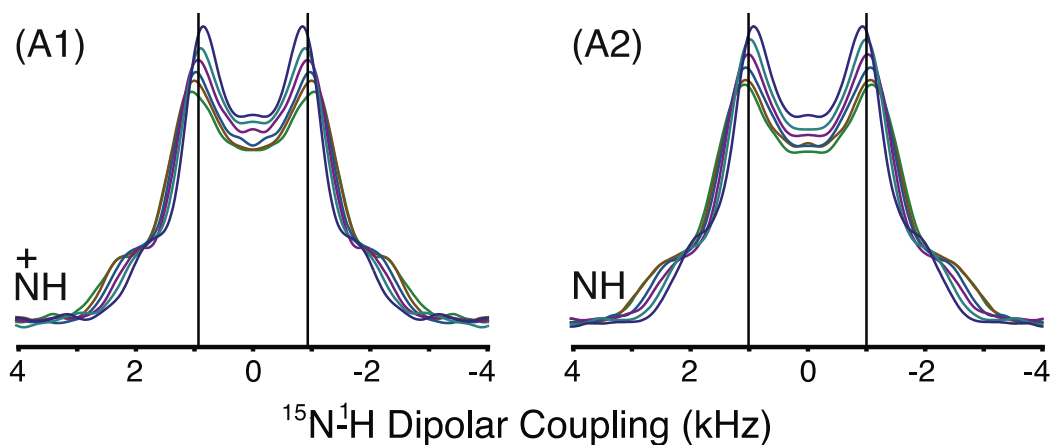


Figure 4: Effect of the rf amplitude mismatch on the ^{15}N - ^1H dipolar coupling powder lineshape of NH^+ and NH groups of imidazole ring of $\text{U-}^{15}\text{N}$ L-His.HCl.H₂O extracted from the 2D ^{15}N - ^1H dipolar coupling/ ^1H CS correlation experiments using the windowless $C3_3^1$ -ROCSA-based DIPSHIFT pulse sequence at the ^1H Larmor frequency of 600 MHz under 69.832 kHz MAS rate. The color scheme in the figure depicts the variation of the ^1H rf amplitudes (green: 80%, brown: 84%, blue: 88%, purple: 92%, light blue: 96% and magenta: 100%) of the symmetry pulses. The calculated ^1H B_1 field ($4\nu_r$ (here ν_r is the MAS rate) = 279.3 kHz) is equal to 92% (vertical lines) of the ^1H rf field strength obtained from the calibration plot (**Figure S6** of the supporting information).

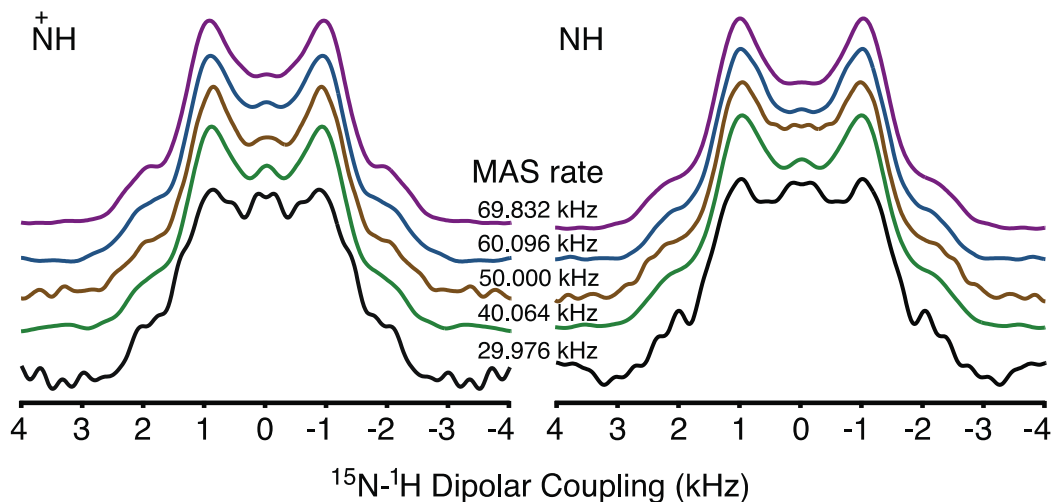


Figure 5: Role of variable MAS rates [29.976 (black), 40.064 (green), 50.000 (brown), 60.096 (blue) and 69.832 (purple) kHz] on the $^{15}\text{N}-^1\text{H}$ dipolar coupling powder lineshape of imidazole's ring NH^+ and NH groups of $\text{U}-^{15}\text{N}$ L-His.HCl.H₂O. The recoupled powder lineshapes are extracted from the 2D $^{15}\text{N}-^1\text{H}$ dipolar coupling ^1H CS correlation experiments using the windowless $C3_3^1$ -ROCSA-based DIPSHIFT pulse sequence at the ^1H Larmor frequency of 600 MHz. Recoupled signals were obtained at every $3\tau_r$ (τ_r : rotor period) for the MAS rates 29.976 (black) and 40.064 (green) kHz, and at every $6\tau_r$ for the MAS rates 50.000 (brown), 60.096 (blue) and 69.832 (purple) kHz.

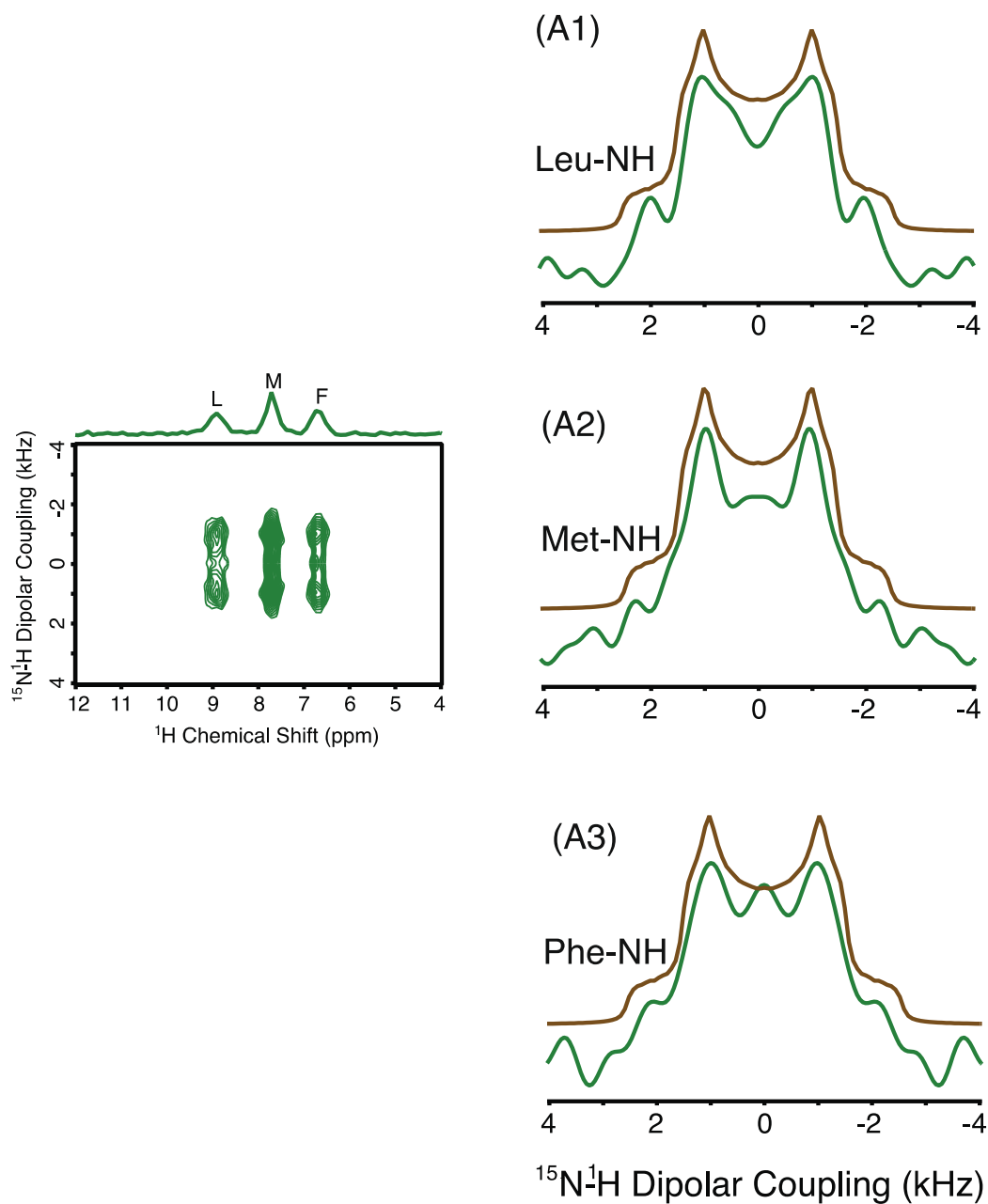


Figure 6: Two-dimensional (2D) ^{15}N - ^1H dipolar coupling/ ^1H CS correlation spectrum (left panel) of naturally abundant MLF recorded by implementing the windowless $C3_3^1$ -ROCSA-based DIPSHIFT pulse sequence at the ^1H Larmor frequency of 899.4 MHz under 60.096 kHz MAS rate. The 2D ^{15}N - ^1H dipolar coupling/ ^1H CS correlation experiment was collected using a recycle delay of 3 s and 32 t_1 time point increments for every 4096 transients. Recoupled signals were obtained at every $3\tau_r$ (τ_r : rotor period) at the rf field strength 240.4 kHz. One-dimensional (1D) projection of the dipolar coupling/CS correlation spectrum is shown onto ^1H CS axis. Experimental (green) ^{15}N -

^1H dipolar coupling powder lineshapes extracted by taking spectral slices parallel the NH dipolar-recoupling dimension of the 2D ^{15}N - ^1H dipolar coupling/ ^1H CS correlation spectrum at the proton isotropic chemical shifts of Leu(L)-NH, Met(M)-NH and Phe(F)-NH resonances are depicted in the right panel. Simulated best-fitted ^{15}N - ^1H dipolar coupling powder lineshapes using a two-spin model from the SIMPSON software are shown in brown. All the simulations were carried out with REPULSION 678 (α, β) crystallite orientations and 60 γ -angles. A single exponential function with a line broadening of 150 Hz was applied before the real Fourier transform of the dipolar modulated time domain data.